Available online at www.sciencedirect.com
ScienceDirect
Trans. Nonferrous Met. Soc. China 21(2011) 2285−2293
Transactions of Nonferrous Metals Society of China
www.tnmsc.cn

Inhomogeneity of density and mechanical properties of A357 aluminum alloy backward extruded in semi-solid state

DU Zhi-ming[1, 2], CHEN Gang[1], CHENG Yuan-sheng[1], XIE Shui-sheng[2]

1. School of Materials Science and Engineering, Harbin Institute of Technology, Harbin 150001, China;
2. State Key Laboratory for Fabrication and Processing of Nonferrous Metals, Beijing General Research Institute for Nonferrous Metals, Beijing 100088, China

Received 00 July 2010; accepted 11 March 2011

Abstract: The inhomogeneity of density and mechanical properties of A357 aluminum alloy in the semi-solid state were investigated. Numerical simulation and backward extrusion were adopted to study the preparation of cup shells. The results show that the relative density of the wall is the lowest in samples, and that of the base is the highest. With increasing the billet height, more time is needed for relative density of the corner to reach the maximum value, and the relative densities in every region improve evidently with increasing the pressure. The tensile stress was simulated to be the largest at the corner, and the hot tearings were forecasted to mainly appear at the corner too. By employing proper billet height and pressure, the extruded samples consisted of fine and uniform microstructures, and can obtain excellent mechanical properties and Brinell hardness.
Key words: A357 aluminum alloy; inhomogeneity; semi-solid state; backward extrusion; numerical simulation

1 Introduction

In recent years, aluminum alloys are widely used in automotive and aerospace industries because of their high specific strength and rigidity. Traditional processing technologies cannot completely satisfy the requirements because forging complex parts is difficult and the casting workpieces cannot obtain excellent properties. Thixoforging is one type of semi-solid metal processing [1−7]. It is no longer a novel, but rather a powerful technology for forming alloys in the semi-solid state to near net shaped products [8−11]. Thixoforging describes the process where suitable material is heated into the semi-solid state and placed into a die to shape the material in the semi-solid state [12−13]. For the alloy to be shaped in the semi-solid state, it must have an appreciable melting range, before thixoforging, the microstructures must consist of solid metal spheroids in a liquid matrix. In this state, the alloy is thixotropic. If it is sheared, the viscosity falls and it flows like liquid; but if allowed to stand it thickens again. The main advantages of thixoforging are low forming temperature (compared with casting) and low forming force (compared with forging) [14−18]. Workpieces with complex shape and excellent mechanical properties could be prepared by thixoforging in one procedure.

Solidification of liquid phase still exists in thixoforging. The deformation and solidification are inhomogeneous because of the applied load and original solid particles, so the microstructures and mechanical properties exhibit obvious inhomogeneity, and even result in hot tearings [19−21].

In this work, the effect of pressure and billet height on true density during backward extrusion process was investigated by numerical simulation (using DEFORM−3D), temperature field and stress field during solidification were investigated by numerical simulation (using ProCAST), and inhomogeneity of mechanical properties and its influencing factor were investigated by extruding cup shells of A357 aluminum alloy in the semi-solid state.

2 Experimental

The composition of A357 aluminum alloy

Foundation item: Projects (50774026, 50875059) supported by the National Natural Science Foundation of China; Project (20070420023) supported by the China Postdoctoral Science Foundation; Project (2008AA03A239) supported by the High-tech Research and Development Program of China
Corresponding author: DU Zhi-ming; Tel: +86-451-86415464; E-mail: duzm@263.net
DOI: 10.1016/S1003-6326(11)61009-1

investigated in this study is provided in Table 1. The solidus and liquidus temperatures of this alloy were obtained as 560 °C and 610 °C using differential thermal analysis (DTA).

Table 1 Composition of A357 aluminum alloy

w(Si)/%	*w*(Mg)/%	*w*(Al)/%	*w*(Ti)/%
6.50−7.50	0.45−0.60	Bal.	≤0.20
w(Fe)/%	*w*(Cu)/%	*w*(Mn)/%	*w*(Zn)/%
≤0.20	≤0.20	≤0.10	≤0.10

2.1 Foundation of simulation model

The density of semi-solid billets alters during thixoforging process because solidification of liquid phase still exists. The semi-solid billets were defined to be rigid-viscoplastic. In this simulation, A357 aluminum alloy was defined as a pseudo-plastic body of porosint. The original relative density was set as 0.96.

The constitutive equation in this simulation is as follows:

$$\bar{\sigma} = \sigma(\varepsilon, \dot{\varepsilon}, T) \tag{1}$$

where $\bar{\sigma}$ is the yield stress, ε is the equivalent strain, $\dot{\varepsilon}$ is the strain rate and T is the temperature. The true stress−true strain responses of A357 semi-solid alloy compressed under different temperatures and strain rates were inputted into material storage, and the flow stress model was established using log-log space linear differential analysis. Figure 1 shows the true stress−true strain response of A357 aluminum alloy compressed at 568, 574 and 580 °C, under the strain rates of 1×10^{-4}, 1×10^{-3}, and 5×10^{-3} s^{-1}, respectively.

Figure 2 shows the geometric model in this simulation, and a half is adopted for its symmetrical character, and the diameter of cup shell is 60 mm. The friction between the billet and the die was described by shear friction model based on the equation of τ=(0.6−0.8)k, where τ is shearing stress and k is shearing yield strength.

2.2 Experimental procedure

Figure 3 shows the schematic diagram of the die of backward extrusion. The extrusion process was performed using a hydraulic press of 2 000 kN. The preheating temperature of the die was 300−350 °C. As-deformed A357 aluminum alloy billets were machined to cylinder-shaped samples with a diameter of 60 mm and different heights. The samples were reheated to 580−590 °C and isothermally held for 40 min using a box type furnace. A hole with a diameter of 1.5 mm was drilled into the centre of each sample, and the temperature of samples was controlled by a K-type

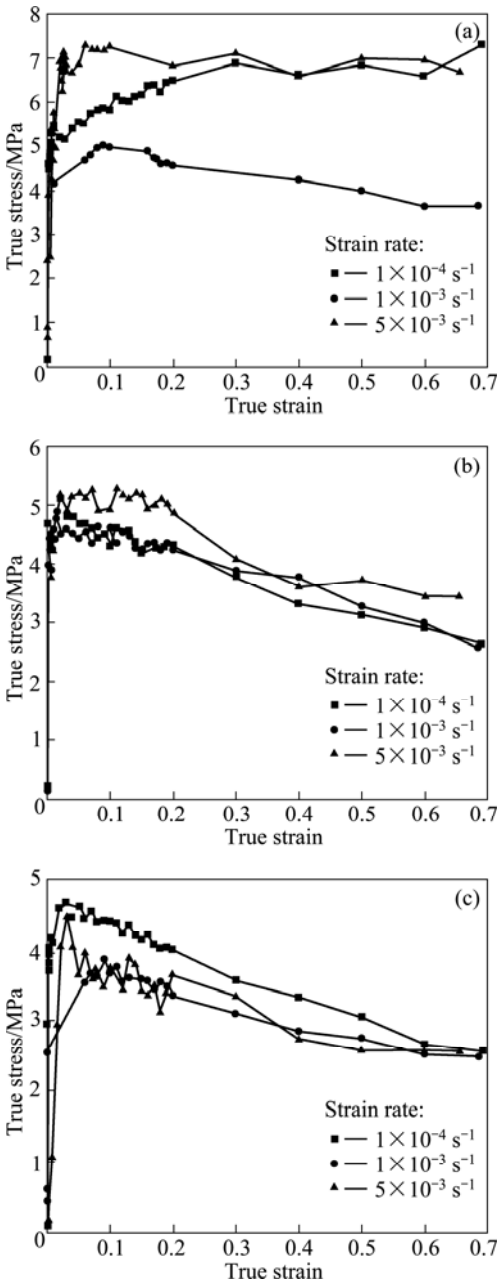

Fig. 1 True stress−true strain response of A357 aluminum alloy compressed at 568 °C (a), 574 °C (b) and 580 °C (c) and at strain rates of 1×10^{-4} s^{-1}, 1×10^{-3} s^{-1}, and 5×10^{-3} s^{-1}

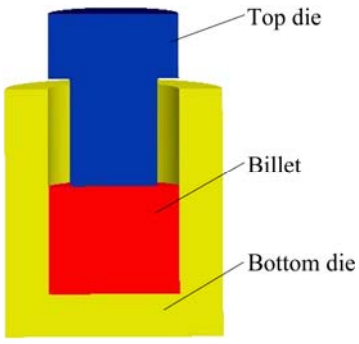

Fig. 2 Geometric model of simulation

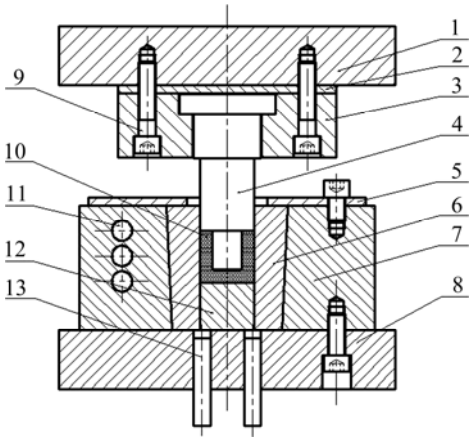

Fig. 3 Schematic diagram of die of backward extrusion: 1—Upper pattern plate; 2—Backing plate; 3—Mounting plate; 4—Upper punch; 5—Pressure back; 6—Bottom die; 7—Die sleeve; 8—Down pattern plate; 9—Screw bolt; 10—Workpiece; 11—Resistance wire; 12—Mould core; 13—Ejector pin

thermocouple inserted in the hole. Graphite was used as lubricant. The loading speed was 15 mm/s and the dwell time was 10−20 s.

The extruded samples were treated under T6 thermal treatment (solution treatment at 490 °C for 3 h plus aging treatment at 160 °C for 10 h). Three different regions of the samples were chosen to be investigated, as shown in Fig. 4. The samples for optical metallography were ground and polished by standard techniques, and then etched for about 20 s with 2.5% HNO_3-1.5% HCl-1% HF aqueous solution [22]. The tensile samples for mechanical property tests were machined from region 1 and region 3 shown in Fig. 4, and were tested using INSTRON 5582 universal testing machine. The true densities of the extruded samples were obtained using Archimedes principle, and the equation for calculating the density is as follows:

$$\rho=\rho_1 m/(m-m_1+ m_2) \quad (2)$$

where m is the tested mass of sample in air; m_1 is the tested mass of sample and hang spring in distilled water; m_2 is the tested mass of hang spring in distilled water; ρ_1 is the density of distilled water at tested temperature. Each tensile or density value is the average of three measurements.

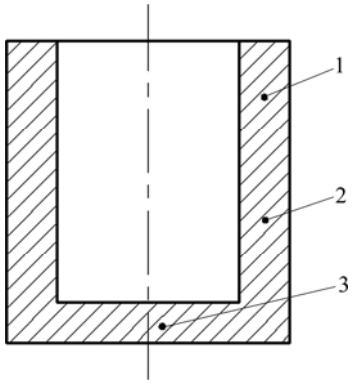

Fig. 4 Different regions for investigation

3 Results and discussion

3.1 Simulation and discussion

Figure 5 shows the relative densities of workpieces extruded under a same pressure of 100 MPa when the billets were 35, 40, 45, 50 and 60 mm in height, respectively.

As shown in Fig. 5(a), P_1 is at the sample wall, P_2 at the corner and P_3 at the base. As shown in Figs. 5 (b)−(f), lines 1, 2 and 3 are the relative densities of P_1, P_2 and P_3, respectively; the relative density of the wall is the lowest in all the samples, and the highest at the base. During the backward extrusion process, the base was compacted heavily since it endured most of pressure, so the relative density was improved obviously at here. With increasing the billet height, more time is needed for relative density of the corner to reach the maximum value. The reason is that friction is playing a more important role with increasing billet height, and more time is needed for overcoming the friction. The separation phenomena of the solid and liquid phase in the thixoforming process were studied (mainly focus on indirect thixoforging), and the marginal region of thixoformed-parts mainly consisted of coarse grains and eutectic network at grain boundaries, resulting in lower mechanical properties and densities compared with those in loading center region [23−25]. However, in this work, the whole semi-solid billets could be applied at a desired pressure in the thixo-extruding process (direct thixoforging). Therefore, the relative density of the firstly-extruded partial wall was improved slightly because the punch applied some load at here.

Figure 6 shows the relative densities of samples extruded under five different pressures (60, 80, 100, 120 and 140 MPa), and with a same billet height of 40 mm.

As shown in Fig. 6(a), P_1 and P_2 are at sample wall, P_3 at the corner and P_4 at the base. As shown in Figs. 6(b)−(f), lines 1, 2, 3 and 4 are the relative densities of P_1, P_2, P_3 and P_4, respectively; the relative densities of every parts were improved with increasing pressure. The relative densities at P_2, P_3 and P_4 reached the maximum value quickly and then presented a stable value, while more time was needed for P_1 to achieve its maximum, and the relative density was always the lowest at P_1 when the pressure was increased from 60 MPa to 120 MPa. The relative densities at P_2, P_3 and P_4 could achieve 0.999 under a small pressure of 80 MPa, but it could only reach 0.998 at P_1 even if a much large pressure of 140 MPa was applied. Figure 6 indicates

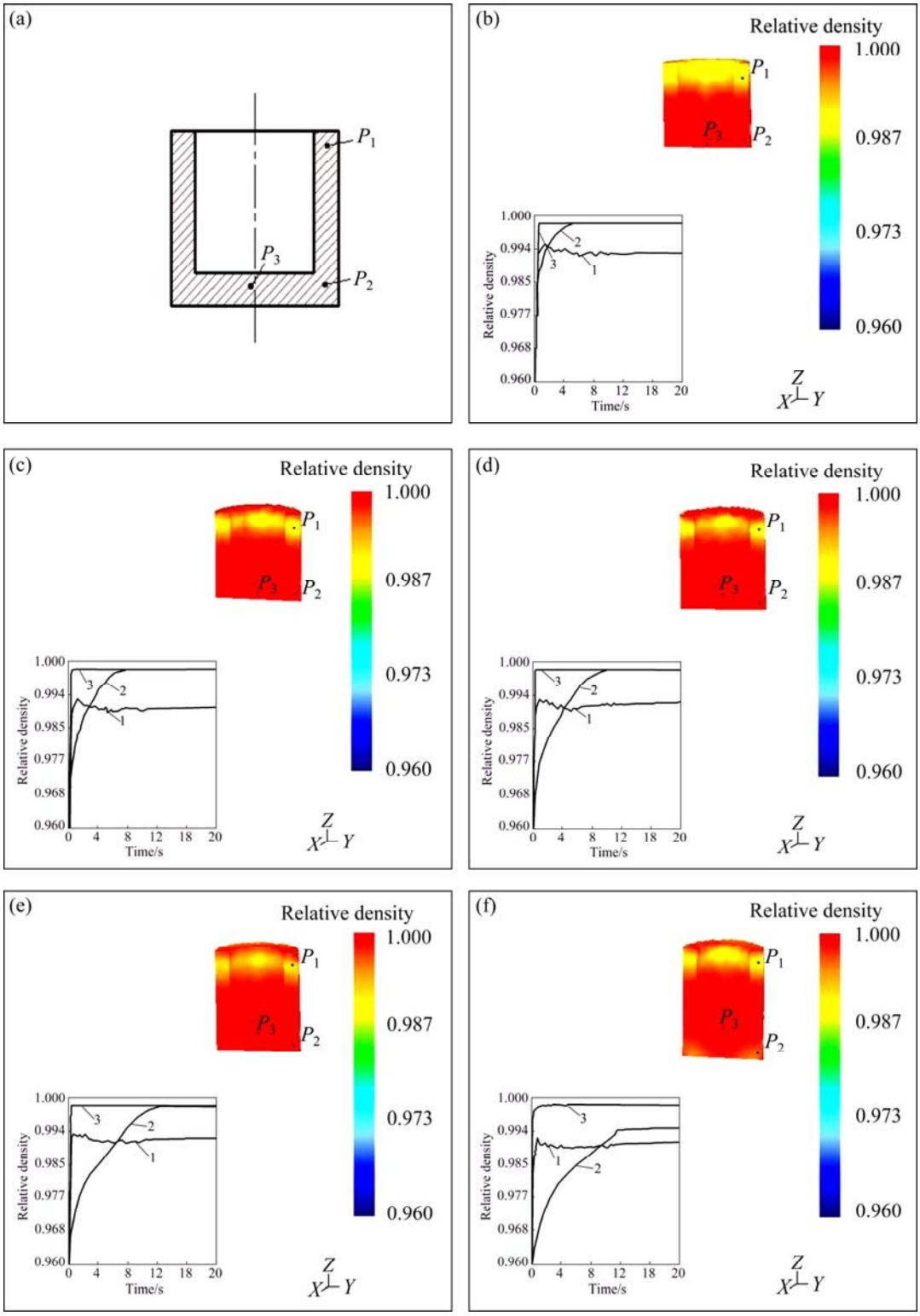

Fig. 5 Positions of characteristic points (a) and relative densities of billets with 35 (b), 40 (c), 45 (d), 50 (e) and 60 mm (f) in height

that the densities were inhomogeneous in backward extruded cup shells due to uneven stress distribution, and a large pressure (>140 MPa) was required for producing a cup shell with uniform densities.

Figure 7 shows the equivalent strain fields during backward extrusion. At the first stage of extrusion process, the deformation was mainly centralized at the corner through where the billets flowed from the base to the wall, and the first-extruded partial wall deformed little because it was similar to inflexible moving, as shown in Figs.7(a) and (b). With the continuing of backward extrusion, as shown in Fig. 7(c), more and

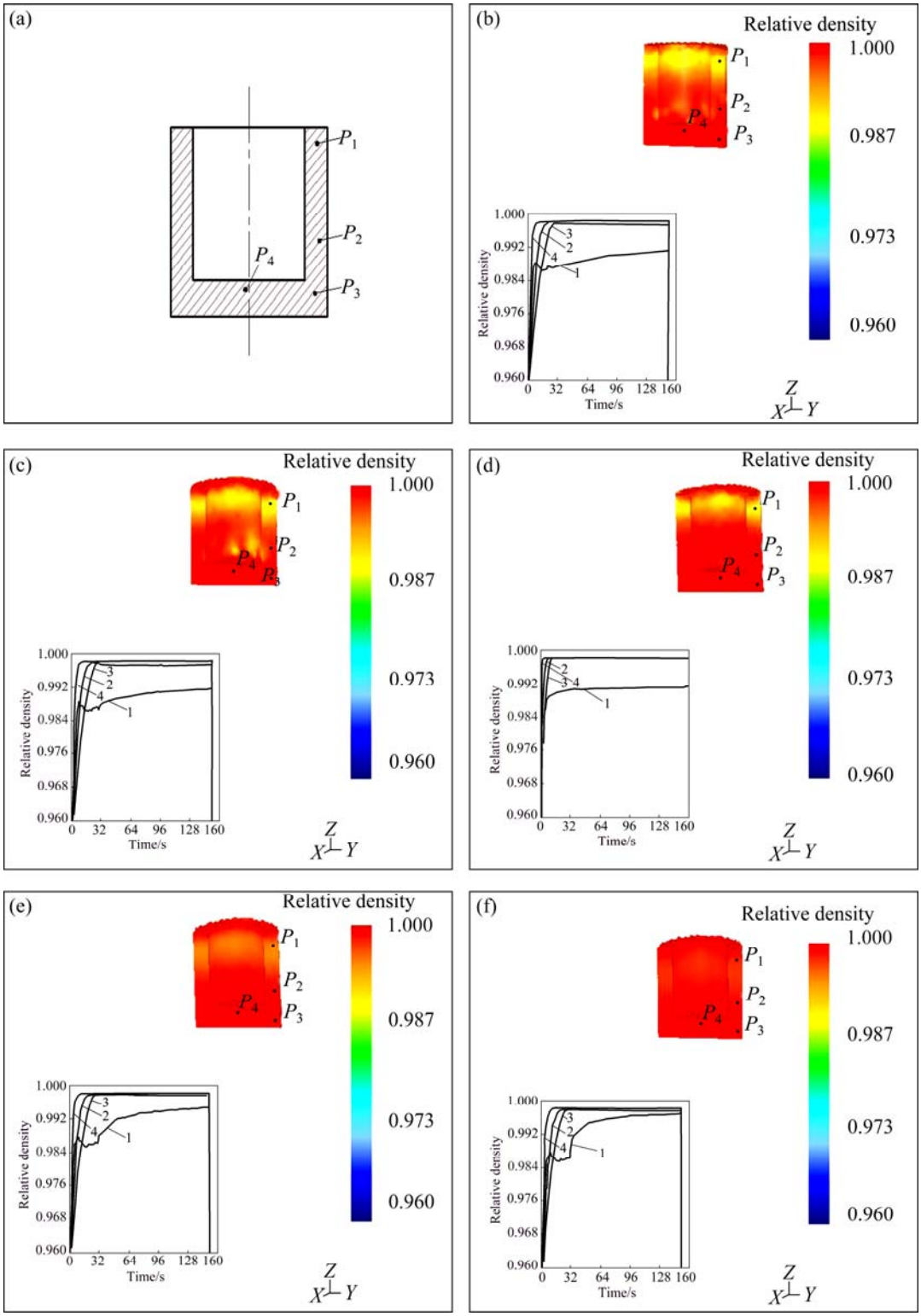

Fig. 6 Positions of characteristic points (a) and relative densities of samples under five different pressures of 60 MPa (b), 80 MPa (c), 100 MPa (d), 120 MPa (e) and 140 MPa (f)

more billets were extruded from the base to the wall, so the deformation was more distributed upon the workpiece, but the equivalent strain was still largest at the corner. At the last stage, as shown in Fig. 7(d), the equivalent strain of the firstly-extruded partial wall increased slightly because the punch applied some load at here. But it was still the lowest, so the density was the lowest at here, as shown in Fig. 5 and Fig. 6.

Figure 8 shows the distribution of fraction of solid at the terminal stage of solidification (billet height of

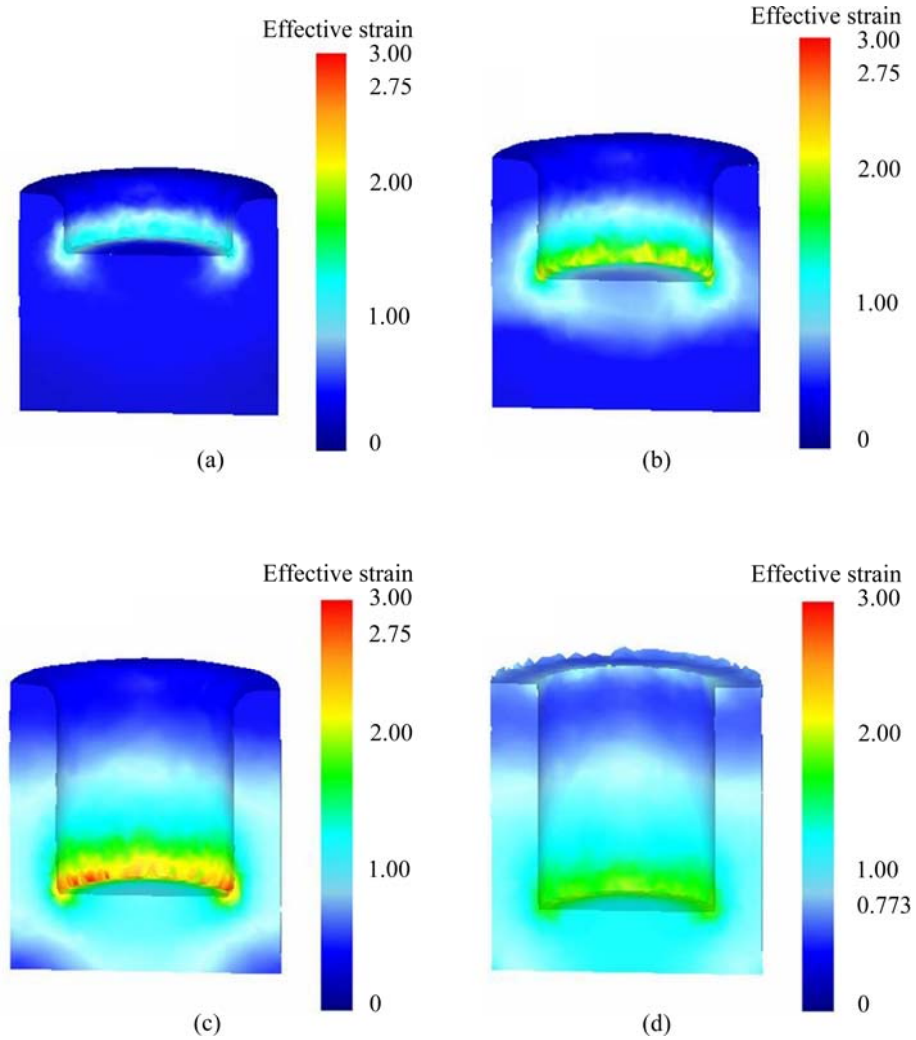

Fig. 7 Equivalent strain fields during backward extrusion: (a) The first stage; (b), (c) Continuing stage; (d) The last stage

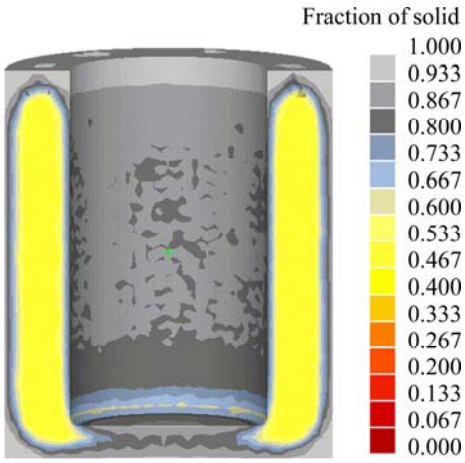

Fig. 8 Distribution of fraction of solid at terminal stage of solidification

60 mm and a pressure of 100 MPa), and the solidification process was simulated using ProCAST. As shown in Fig. 8, the fraction of solid is the lowest in the wall, indicating that some liquid alloy still existed at here while the solidification had almost finished at the base. The solidified alloy cannot obtain enough liquid feeding from solidified material, and considerable tensile stress may be aroused due to solidification shrinkage.

Figure 9 shows the distribution of the first principal stress in the terminal stage of solidification. As shown in Fig. 9, the tensile stress is the largest at the corner. The reason is attributed to the thermal stress caused by solidification shrinkage of the wall, in combination with the limited liquid feeding from the base. The hot tearings would appear probably in the region where the thermal stress surpasses the tensile strength, in combination with limited liquid feeding and low ductility. As shown in Fig. 10, the hot tearings were forecasted to mainly appear in the yellow region at the corner.

3.2 Results and discussion

Figure 11 shows the extruded cup shells prepared with different billets heights and under different pressures.

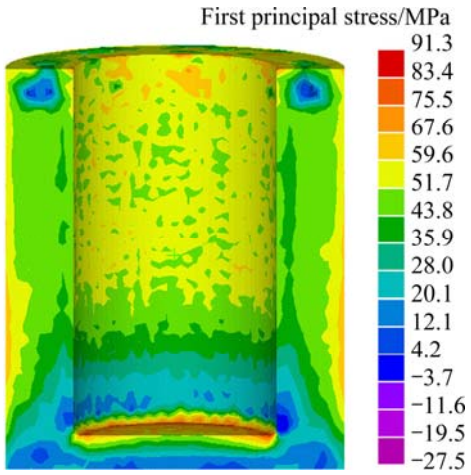

Fig. 9 Distribution of the first principal stress in terminal stage of solidification

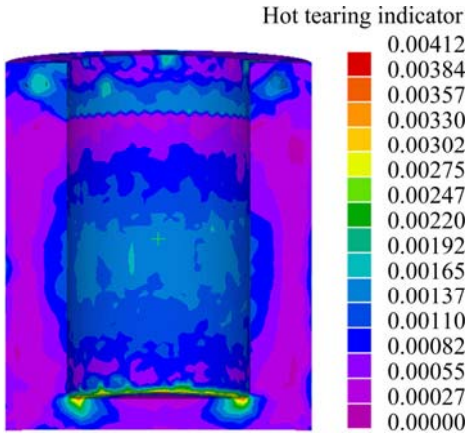

Fig. 10 Forecast of distribution of hot tearings

Fig. 11 Extruded cup shells prepared with different billets heights (a) and under different pressures (b)

Figure 12 shows the true densities of the extruded cup shells prepared with different billets heights (under a same pressure of 100 MPa), and under different pressures (with a same billet height of 40 mm). As indicated in Fig. 12(a), the true densities in regions 1, 2 and 3 all decreased with increasing billet height, and the density was always the highest in region 3 and lowest in region 1. For billet with 35 mm in height, the true densities in the three different regions were almost uniform, and appeared more inhomogeneous with increasing billet height. When the billet height was too high, the pressure would overcome more friction, and the semi-solid billets could not be compacted sufficiently. The testing results were anastomotic to the simulation, and higher pressure was needed for extruding workpieces of high-height. As shown in Fig. 12(b), the true densities of regions 1, 2 and 3 all increased with increasing the pressure, and the density was always the highest in region 3 and lowest in region 1. The true density in region 1 was still lower than that in region 3 slightly, even when the pressure of 140 MPa was applied. The testing results were anastomotic to the simulation too, indicating that higher pressure (more than 140 MPa) was needed for preparing backward extruded workpieces with uniform density.

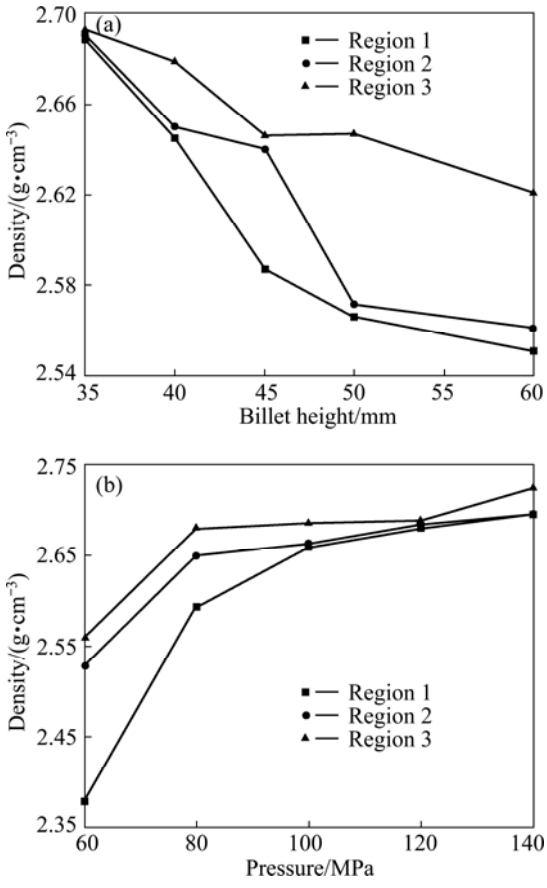

Fig. 12 True densities of extruded cup shells prepared by billets with different heights (a) and under different pressures (b)

Figure 13 shows the microstructures in different regions of the extruded cups (a billet height of 40 mm and a pressure of 140 MPa). As shown in Fig. 13, the microstructures are very fine with grain sizes of 20−50 μm. The extruded samples consisted of fine and uniform

microstructures.

The mechanical properties and Brinell hardness were tested in regions 1 and 3 (a billet height of 40 mm and a pressure of 140 MPa), as shown in Table 2. The extruded samples could obtain excellent mechanical properties and Brinell hardness, and they were slightly higher in the region 3 than those in region 1.

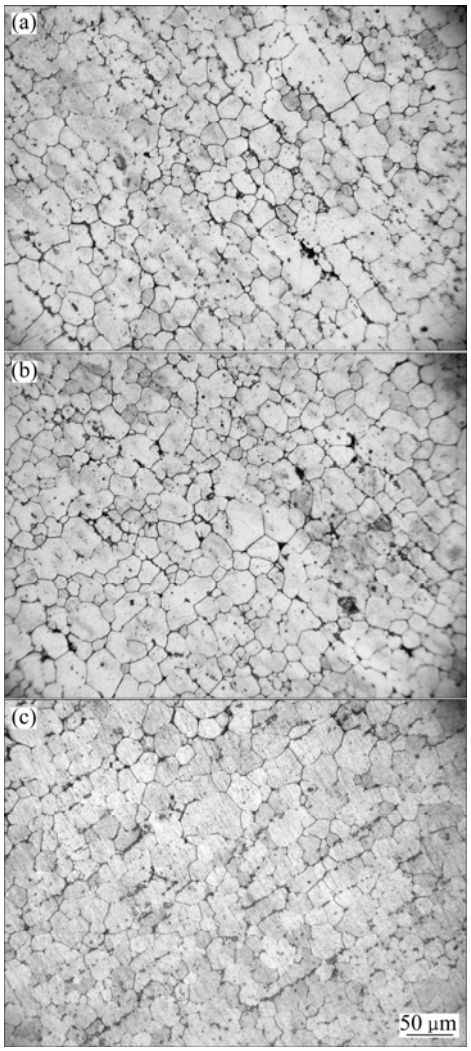

Fig. 13 Microstructures of extruded cup shell in regions 1 (a), 2 (b) and 3 (c)

Table 2 Mechanical properties and Brinell hardness tested in regions 1 and 3

Region	Tensile strength/ MPa	Yield stress/ MPa	Elongation/ %	Brinell hardness, HBS
1	383	310	9.0	155
3	391	315	8.8	172

4 Conclusions

1) For cup shells backward extruded in the semi-solid state, the relative density of the wall was the lowest, and the highest at the base. With increasing the billet height, more time was needed for relative density of the corner to reach the maximum value. The relative densities of every parts were improved with increasing pressure, and a large pressure (>140 MPa) was required for producing a cup shell with uniform densities.

2) In the terminal stage of solidification, tensile stress distributed upon the extruded cup shells unevenly, and was the largest at the corner. The hot tearings were forecasted to mainly appear at the corner.

3) The experimental results were anastomotic to the simulation, and backward extruded workpieces could obtain high and uniform densities with lower billet height and higher pressure. The extruded samples consisted of fine and uniform microstructure, and could obtain excellent mechanical properties (tensile strength of 380 MPa and elongation of 9.0%) and Brinell hardness (HBS of 150), if employing proper billets height and pressure.

References

[1] OMAR M Z, PALMIERE E J, HOWE A A, ATKINSON H V, KAPRANOS P. Thixoforming characteristics of thermomechanically treated AA6061 alloy for suspension parts of electric vehicles [J]. Journal of Materials Processing Technology, 2002, 130−131: 587−593.

[2] KAPRANOS P, WARD P J, ATKINSON H V, KIRKWOOD D H. Near net shaping by semi-solid metal processing [J]. Materials & Design, 2000, 21: 387−394.

[3] ZHAO Z D, CHEN Q, HU C K, HUANG S H, WANG Y Q. Near-liquidus forging, partial remelting and thixoforging of an AZ91D+ Y magnesium alloy [J]. Journal of Alloys and Compounds, 2009, 485: 627−636.

[4] COLEA E T, CADEB D, BENAMEUR H. Challenges and opportunities in the encapsulation of liquid and semi-solid formulations into capsules for oral administration [J]. Advanced Drug Delivery Reviews, 2008, 60(6): 747−756.

[5] LUO S J, CHEN Q, ZHAO Z D. Effects of processing parameters on the microstructure of ECAE-formed AZ91D magnesium alloy in the semi-solid state [J]. Journal of Alloys and Compounds, 2009, 477: 602−607.

[6] PARK H N, GOVENDER G, IVANCHEV L. Opportunities and challenges for use of SSM forming in the aerospace industry [J]. Solid State Phenomena, 2006, 116−117: 92−95.

[7] CHEN Q, LUO S J, ZHAO Z D. Microstructural evolution of previously deformed AZ91D magnesium alloy during partial remelting [J]. Journal of Alloys and Compounds, 2009, 477: 726−731.

[8] KIRKWOOD D H. Encyclopedia of materials: Semisolid processing [M]. New York: Elsevier Publishers, 2008: 8432−8437.

[9] JORSTAD J L. Encyclopedia of materials: Casting of semisolid metals [M]. New York: Elsevier Publishers, 2008: 1016−1020.

[10] ZHAO Z D, CHEN Q, HUANG S H, CHAO H Y. Microstructural evolution and tensile mechanical properties of thixoforged ZK60-Y magnesium alloys produced by two different routes[J]. Materials and Design, 2010, 31: 1906−1916.

[11] ZHAO Zu-de, CHEN Qiang, WANG Yan-bin, SHU Da-yu. Effect of predeformation on semi-solid microstructure of ZK60+RE magnesium alloy [J]. Transaction of Nonferrous Metals Society of

China, 2009, 19: 535−539.
[12] WITULSKI T, HEUBEN J M M, WINKELMANN A, HIRT G, KOPP R. Near net shape forming of particulate reinforced Al-alloys by isothermal forming compared to semi solid forming [J]. Journal of Materials Processing Technology, 1994, 45(1−4): 415−420.
[13] ATKINSON H V. Modelling the semisolid processing of metallic alloys [J]. Progress in Materials Science, 2005, 50(3): 341−342.
[14] WALLACE G, JACKSON A P, MIDSON S P, ZHU Q. High-quality aluminum turbocharger impellers produced by thixocasting [J]. Transactions of Nonferrous Metals Society of China, 2010, 20: 1786−1791.
[15] ZHAO Zu-de, CHENG Yuan-sheng, CHEN Qiang, WANG Yan-bin, SHU Da-yu. Reheating and thixoforging of ZK60+RE alloy deformed by ECAE [J]. Transaction of Nonferrous Metals Society of China, 2010, 20(2): 178−182.
[16] CHENG Yuan-sheng, CHEN Qiang, HUANG Zhe-qun, HUANG Shu-hai. Microstructure evolution and thixoextrusion of AZ91D magnesium alloy produced by SSTT [J]. Transaction of Nonferrous Metals Society of China, 2010, 20(s3): s739−s743.
[17] ZHAO Zu-de, CHEN Qiang, HUANG Shu-hai, KANG Feng, WANG Yan-bin. Microstructure and tensile properties of AM50A magnesium alloy prepared by recrystallisation and partial melting process[J]. Transaction of Nonferrous Metals Society of China, 2010, 20(9): 1630−1637.
[18] LUO Shou-jing, KEUNG W C, KANG Yong-lin. Theory and application research development of semi-solid forming in China [J]. Transactions of Nonferrous Metals Society of China, 2010, 20: 1805−1814.
[19] DU Z M, SHAN W W, CUI Y T, PENG Q C. Numerical simulation of pressure influence on workpiece properties during thixoforging [J]. Solid State Phenomena, 2006, 116−117: 167−172.
[20] PHILLION A B, COCKCROFT S L, LEE P D. A new methodology for measurement of semi-solid constitutive behavior and its application to examination of as-cast porosity and hot tearing in aluminum alloys [J]. Material Science and Engineering A, 2008, 491: 237−247.
[21] DU Zhi-ming, CHEN Gang, LIU Jun, XIE Shui-sheng. Tensile properties of as-deformed 2A50 aluminum alloy in semi-solid state [J]. Transactions of Nonferrous Metals Society of China, 2010, 20(9): 1597−1602.
[22] de FREITAS E R, FERRACINI E Jr, FERRANTE M. Microstructure and rheology of an AA2024 aluminium alloy in the semi-solid state, and mechanical properties of a back-extruded part [J]. Journal of Materials Processing Technology, 2004, 146(2): 241−249.
[23] CHO W G, KANG C G. Mechanical properties and their microstructure evaluation in the thixoforming process of semi-solid aluminum alloys [J]. Journal of Materials Processing Technology, 2000, 105: 269−277.
[24] KIM N S, KANG C G. An investigation of flow characteristics considering the effect of viscosity variation in the thixoforming process [J]. Journal of Materials Processing Technology, 2000, 103: 237−246.
[25] SEO P K, YOUN S W, KANG C G. The effect of test specimen size and strain-rate on liquid segregation in deformation behavior of mushy state material [J]. Journal of Materials Processing Technology, 2002, 130−131: 551−557.

半固态反挤压 A357 铝合金的力学性能及其密度的不均匀性

杜之明[1,2], 陈 刚[1], 程远胜[1], 谢水生[2]

1. 哈尔滨工业大学 材料科学与工程学院，哈尔滨 150001；
2. 北京有色金属研究总院 有色金属制造与加工国家重点实验室，北京 100088

摘 要：通过数值模拟及反挤压成形对半固态 A357 铝合金的密度及力学性能的不均匀性进行研究。结果表明：反挤压制件直壁部的相对密度最小，底部的最大。随着坯料高度的增加，转角处的相对密度需要更长的时间才能达到最高值；随着压力的增加，制件各部的相对密度均增加。模拟结果表明，制件的转角处的拉应力最大，该处产生热裂纹的可能性也最大。通过采用合适的坯料高度及压力，半固态挤压件能够获得细小、均匀的微观组织，且能达到优良的力学性能及硬度。

关键词：A357 铝合金；不均匀性；半固态；反挤压；数值模拟

(Edited by YANG Hua)